BMC Cardiovascular Disorders

RESEARCH

Open Access

The role and possible mechanism of the ferroptosis-related SLC7A11/GSH/GPX4 pathway in myocardial ischemia-reperfusion injury

Bingxin Chen[1,3], Ping Fan[1], Xue Song[1] and Mingjun Duan[2*]

Abstract

Background Myocardial ischemia-reperfusion injury (MI/RI) is an unavoidable risk event for acute myocardial infarction, with ferroptosis showing close involvement. We investigated the mechanism of MI/RI inducing myocardial injury by inhibiting the ferroptosis-related SLC7A11/glutathione (GSH)/glutathione peroxidase 4 (GPX4) pathway and activating mitophagy.

Methods A rat MI/RI model was established, with myocardial infarction area and injury assessed by TTC and H&E staining. Rat cardiomyocytes H9C2 were cultured in vitro, followed by hypoxia/reoxygenation (H/R) modeling and the ferroptosis inhibitor lipoxstatin-1 (Lip-1) treatment, or 3-Methyladenine or rapamycin treatment and overexpression plasmid (oe-SLC7A11) transfection during modeling. Cell viability and death were evaluated by CCK-8 and LDH assays. Mitochondrial morphology was observed by transmission electron microscopy. Mitochondrial membrane potential was detected by fluorescence dye JC-1. Levels of inflammatory factors, reactive oxygen species (ROS), Fe^{2+}, malondialdehyde, lipid peroxidation, GPX4 enzyme activity, glutathione reductase, GSH and glutathione disulfide, and SLC7A11, GPX4, LC3II/I and p62 proteins were determined by ELISA kit, related indicator detection kits and Western blot.

Results The ferroptosis-related SLC7A11/GSH/GPX4 pathway was repressed in MI/RI rat myocardial tissues, inducing myocardial injury. H/R affected GSH synthesis and inhibited GPX4 enzyme activity by down-regulating SLC7A11, thus promoting ferroptosis in cardiomyocytes, which was averted by Lip-1. SLC7A11 overexpression improved H/R-induced cardiomyocyte ferroptosis via the GSH/GPX4 pathway. H/R activated mitophagy in cardiomyocytes. Mitophagy inhibition reversed H/R-induced cellular ferroptosis. Mitophagy activation partially averted SLC7A11 overexpression-improved H/R-induced cardiomyocyte ferroptosis. H/R suppressed the ferroptosis-related SLC7A11/GSH/GPX4 pathway by inducing mitophagy, leading to cardiomyocyte injury.

Conclusions Increased ROS under H/R conditions triggered cardiomyocyte injury by inducing mitophagy to suppress the ferroptosis-related SLC7A11/GSH/GPX4 signaling pathway activation.

*Correspondence:
Mingjun Duan
mingjunD_urmq@163.com

Full list of author information is available at the end of the article

Keywords Myocardial ischemia-reperfusion injury, Ferroptosis, The SLC7A11/GSH/GPX4 pathway, Mitophagy, SLC7A11, Lipid peroxidation, Membrane potential, GPX4 enzyme

Background

Myocardial ischemia-reperfusion injury (MI/RI) is a disorder that causes structural damage, myocardial dysfunction, and electrical activity disturbances following coronary blood flow recovery in patients with ischemic heart disease, resulting in a significant spik in myocardial infarction mortality [1, 2]. Reperfusion of ischemic tissues facilitated the elevation of mitochondrial reactive oxygen species (ROS), which causes cardiac cell death and irreparable damage to the heart muscle [3].

Accumulating reports reveal that programmed cell death such as necrosis, apoptosis, pyroptosis, and autophagic cell death all participate in the occurrence and development of MI/RI [4–7]. Notably, ferroptosis is a form of cell death that occurs owing to ferrous ion buildup, which triggers intracellular lipid peroxidation (LPO) through the Fenton reaction [8]. Presently, ferroptosis inhibitors have demonstrated cardioprotective benefits against MI/RI [9, 10]. For instance, it is reported that fucoxanthin mitigates MI/RI by repressing the ferroptosis nuclear factor erythroid-2 related factor 2 (Nrf2) pathway [11]. DYRK1a exacerbates MI/RI progression by mediating cardiomyocyte ferroptosis [3]. Although the aforementioned research indicates a strong correlation between ferroptosis and MI/RI pathogenesis and progression, the specific molecular mechanisms of ferroptosis in MI/RI progression remain elusive. Furthermore, system Xc-/glutathione (GSH)/glutathione peroxidase 4 (GPX4) is one of the pathways regulating ferroptosis [12]. SLC7A11 facilitates cystine absorption and promotes GSH production, thereby reducing oxidative damage [13, 14]. There is proof that naringenin can suppress ferroptosis by modulating the Nrf2/system Xc-/GPX4 pathway, thereby mitigating MI/RI [1]. The SGLT2 inhibitor dapagliflozin prevents ferroptosis by upregulating the SLC7A11/GPX4 axis and ferritin heavy chain to curb acyl-CoA synthetase long chain family member 4 [15]. Moreover, autophagy, an evolutionarily conserved mechanism, is degraded in organelles and macromolecular cells [16]. NIX, a receptor of mitophagy, can release beclin1 and trigger mitophagy, and it can hinder the function of system Xc- and suppress ferroptosis by binding to SLC7A11, implying a potential connection between ferroptosis and mitophagy [17]. It has recently been proposed that there is an interplay between selective autophagy and ferroptosis in a ROS-dependent manner [18]. GPX4 may initiate hepatocyte ferroptosis via mitophagy and the destruction of mitochondria caused by ROS-induced damage [19]. Nevertheless, whether the ferroptosis-related SLC7A11/GSH/GPX4 pathway activates mitophagy to play a role in MI/RI remains elusive. As reported, cardiomyocyte injury induced by in vitro hypoxia/reoxygenation (H/R) and in vivo MI/RI is essentially identical; in fact, the majority of cell-level research on in vivo MI/RI is based on the in vitro H/R-stimulated cardiomyocytes [20, 21]. In this study, we established in vitro and in vivo models and focused on whether the ferroptosis-associated SLC7A11/GSH/GPX4 pathway induced MI/RI by activating mitophagy, so as to provide a new therapeutic target for MI/RI.

Methods

Ethics statement

All experimental protocols were reviewed and approved by the Research and Ethics Committee of the First Affiliated Hospital of Xinjiang Medical University. All procedures conformed to internationally accepted guidelines and ethics for animal research. All authors confirm that all methods are reported in accordance with ARRIVE guidelines for the reporting of animal experiments. Great efforts were made to reduce the total number of animals used and to minimize their suffering.

Establishment of MI/RI rat model and grouping

A total of 24 male Sprague-Dawley rats (12 weeks old, weighing 230±20 g, Urumqi, Xinjiang One Molecular Biotechnology Co., LTD) were fed at 24±2 °C, with 50±10% humidity, in a 12-h light/dark cycle. After one week of adaptive feeding, rats were randomly allocated to two groups (n=12 per group), including the Sham group and the MI/R group. Rats in the MI/R model received intraperitoneal anesthesia with 1% pentobarbital sodium (60 mg/kg). Later, rats were mechanically ventilated using an animal ventilator after tracheal intubation. The heartbeat and typical electrocardiogram alteration at the initiation of MI were monitored using a three-lead electrocardiogram. During the surgery, a microcatheter (Taimeng Technology, Chengdu, Sichuan, China) was inserted into the left ventricle via the right carotid artery, in a bid to evaluate cardiac function. The left anterior descending coronary artery was ligated by a sliding node for 30 min to induce MI, followed by myocardial reperfusion for 4 h. The same surgical method was adopted in the Sham groupwith no need for ligation. White coloration of the left ventricular apex and anterior wall indicated successful model induction and recovery of redness of the left ventricular apex and anterior wall indicated successful reperfusion [1].

After the end of the experiment, rats were euthanized using 1% pentobarbital sodium (200 mg/kg) before being

dissected for collection of heart tissues. The heart tissues of six rats in each group were immediately frozen at -20 °C for 2,3,5-triphenyl tetrazolium chloride (TTC) staining. Half of the heart tissues of another six rats were immobilized in 4% tissue fixative and made into paraffin sections for hematoxylin and eosin (H&E) staining, and the half remaining heart tissues were prepared into tissue homogenates and stored at -80 °C for enzyme-linked immunosorbent assay (ELISA) and Western blot assay.

TTC staining

Myocardial tissues were collected, rapidly frozen at -20 °C for about 20 min, and cut into sections at 1 mm intervals. Next, tissue sections were removed at 1 mm intervals, followed by staining in TTC at a concentration of 2% without light for 20 min at 37 °C. Thereafter, sections were subjected to fixation in 4% paraformaldehyde for 24 h and photographed. The Image Pro Plus 6.0 software was used for image analysis [1].

H&E staining

The tissues were fixed in 4% paraformaldehyde for 24 h. Then, the tissue samples were embedded in paraffin, cut into sections at 4 μM thickness, and stained with H&E staining according to the protocol. After five fields of view were randomly selected, the histopathological changes were under observation using a microscope (Olympus, Tokyo, Japan) [1].

Cell culture

Rat cardiomyocytes (H9C2) (FH1004) and H9C2 complete culture medium (FH-H9C2) (Fuheng Biology, Shanghai, China) were cultured and passaged in an incubator at 37 °C, with 5% CO_2 and 95% humidity.

Cell H/R treatment and grouping

H9C2 cells were exposed to a high-glucose (35 mM glucose) medium for 48 h, followed by hypoxia treatment in a glucose- and fetal bovine serum-free medium. After 8-h hypoxia treatment, H9C2 cells were re-oxygenated in the high-glucose medium for 12 h, and cells were harvested [22].

According to different treatments, cells were categorized into the following 10 groups: (1) the Con group (normally cultured H9C2 cells); (2) the H/R group (establishment of the H/R model on H9C2 cells); (3) the H/R+Lip-1 group [simultaneous treatment with H/R and liproxstatin-1 (Lip-1) (a ferroptosis inhibitor; SML1414, Sigma, St Louis, MO, USA) on H9C2 cells [23]]; (4) the H/R+DMSO group [H9C2 cells were treated with H/R and the equivalent amount of dimethyl sulfoxide (DMSO, a Lip-1 solvent)]; (5) the H/R+oe-NC group (H9C2 cells underwent oe-NC transfection); (6) the H/R+oe-SLC7A11 group (H9C2 cells were delivered with oe-SLC7A11); (7) the H/*R*+3-MA group [H9C2 cells were cultured with 3-Methyladenine (3-MA, an autophagy inhibitor; 5142-23-4, MCE, Monmouth Junction, NJ, USA) [24]]; (8) the H/R+DMSO group (H9C2 cells were treated with the same amount of 3-MA solvent DMSO); (9) the H/R+oe-SLC7A11+RA group (H9C2 cells were subjected to treatment with oe-SLC7A11 and rapamycin solvent (an autophagy activator; 553210, Sigma) [25]]; (10) the H/R+oe-SLC7A11+DMSO group (H9C2 cells received oe-SLC7A11 transfection and DMSO (a rapamycin solvent) treatment.

Using Lipofectamine®2000 (Invitrogen, Carlsbad, CA, USA), pcDNA3.1-SLC7A11 (oe-SLC7A11) and its corresponding negative control pcDNA3.1-NC (oe-NC) (GenePharma, Shanghai, China) were introduced into H9C2 cells at a concentration of 100 ng/μL. Subsequently, cells were treated with 1 μM Lip-1, 2 mM 3-MA, or 100 nM rapamycin and their equivalent corresponding solvents for 24 h, respectively [23, 24, 26, 27]. The specific operation was carried out as per the instructions.

Cell counting kit-8 (CCK-8) assay

Differently treated cells were seeded onto 96-well plates at 5×10^3 cells/well. Cell viability was assayed at 0, 6, 12, and 24 h using the CCK-8 kit (CA1210, Solarbio). Cells were cultivated at 37 °C for 2 h after the addition of 100 μL/well CCK-8 working solution in each well. The measurement of optical density (OD) value at 450 nm was performed using a microplate reader (Thermo Fisher Scientific).

Lactate dehydrogenase (LDH) assay

Cell toxicity was quantified using an LDH assay kit (A020-2-2, Jiancheng Bioengineering Institute, Nanjing, Jiangsu, China). As per the given instructions, the supernatant was collected after cells were subjected to centrifugation at 600 g and 4 °C for 5 min. The working solution of this reagent kit was sequentially put onto the 96 well plates, and the samples were incubated at 37 °C for 30 min. The OD value was measured at 450 nm. The specific experimental steps were under the instructions [28].

ELISA

Levels of interleukin (IL)-6, tumour necrosis factor alpha (TNF-α) and IL-1β were determined utilizing the ELISA kits (IL-6, Cat. No. ERC003QT.96; TNF-α, Cat. No. ERC102aQT.48; IL-1β, Cat. No. EMC001b.96.2) as per the instructions for the specific experimental steps. All reagent kits were obtained from NeoBioscience (Shenzhen, Guangdong, China).

ROS measurement

The cell ROS detection kit was purchased from Abcam (ab186029, Cambridge, MA, USA). The specific experimental steps were carried out following the manuals.

Determinations of Fe^{2+}, malondialdehyde (MDA), LPO, GPX4 enzyme activity, glutathione reductase (GR), GSH and glutathione disulfide(GSSG)

Levels of Fe^{2+}, MDA, LPO, GPX4 enzyme activity, GSH, GR and GSSG were measured using the iron assay kit (ab83366, Abcam), MDA assay kit (ab118970, Abcam), LPO assay kit (ab133085, Abcam), GPX4 enzyme activity assay kit (CB12629-Ra, COIBO BIO, Shanghai, China), reduced GSH assay kit (BC1175, Solarbio, Beijing, China), GR assay kit (LZ-01372 S, Lianzu Biotechnology Co., Ltd., Shanghai, China) and GSSG assay kit (ab239709, Abcam), respectively referring to the manufacturer's manual.

Western blot

Cells and tissues were gathered from each group respectively, and supplemented with cell lysate to extract proteins. The protein concentration was determined using a bicinchoninic acid assay kit (AR1189, Boster Biological Technology, Wuhan, Hubei, China). Later, an appropriate amount of loading buffer was added to the protein samples, and the mixture was heated in a boiling water bath for 5 min to induce protein denaturation. The denatured protein samples were then placed into the upper sample hole. SDS-PAGE electrophoresis was performed, and the proteins were separated and electrotransferred to a PVDF membrane for transmodeling, and then placed in BSA containing 3% for 2 h. Subsequently, samples were incubated with anti-GPX4 (1:1000, #59735, CST, Danvers, MA, USA), anti-SLC7A11 (1:1000, #98051, CST), anti-LC3II/I (1:1000, #43566, CST), and anti-p62 (1:1000, #5114, CST) overnight at 4 °C, with β-actin (1:1000, #4967, CST) as the internal reference. Afterward, the samples interacted with the horseradish peroxidase-labeled secondary antibody (1:2000, BA1054, Boster Biological Technology) at room temperature in the dark for 1 h, and then subjected to color development in enhanced chemiluminescence working solution (AR1191, Boster Biological Technology). The grayscale of each band was quantified in Western blot images using Image Pro Plus 6.0 (Media Cybernetics, Bethesda, MD, USA). The experiment was repeated three times.

Transmission electron microscopy (TEM)

Cells were fixed at room temperature for 3 h with 2.5% glutaraldehyde (Sigma) before being washed with phosphate-buffered saline at pH 7.4. Thereafter, cells were fixated in 1% osmic acid for 1.5 h, followed by gradient dehydration in 50%, 70%, 80%, 90% ethanol, 90% acetone, and pure acetone. After penetration with acetone and resin, cells were embedded with resin, and the thickness of sections was 70 nm. BAF and DMSO were added 4 h before cell fixation. Mitochondrial morphology was viewed using a TEM (HT-7800, Hitachi, Japan) [29].

Mitochondrial membrane potential (MMP) determination

MMP was quantified using fluorescent probe JC-1 (ab113850, Abcam) following the given directions. Cells were plated in the 6-well plates at a seeding density of 1×10^6 cells/well, stained with JC-1, centrifuged, and washed. The fluorescence intensity was measured utilizing a fluorescence microscope (Olympus) [30].

Statistical analysis

Data from this study were statistically analyzed and graphed using SPSS 21.0 (IBM, Armonk, NY, USA) and GraphPad Prism 8.01 (GraphPad, San Diego, CA, USA) statistical software. The normal distribution of continuous variables was validated by Kolmogorov-SmiRnov. The data that conformed to the normal distribution were expressedas mean ± standard deviation. The independent sample *t*-test was used to compare data between the two groups, and one-way analysis of variance (ANOVA) was implemented to compare data among groups, followed by Tukey's multiple comparison test. The difference was statistically significant with $P<0.05$.

Results

I/R inhibited ferroptosis-related SLC7A11/GSH/GPX4 pathway and induced myocardial injury

We established an MI/RI rat model following the previous method [1]. Compared with the Sham group, the MI/R group had an increased myocardial infarction area (Fig. 1A). Myocardial injury was assessed by H&E staining, and there was more severe myocardial injury in the MI/R group than in the Sham group (Fig. 1B). Besides, ELISA elicited that the expression levels of TNF-α, IL-6 and IL-1β in the MI/R group were up-regulated relative to the Sham group (Fig. 1C, all $P<0.01$). In comparison with the Sham group, the MI/R group exhibited decreased GR and GSH levels and increased Fe^{2+} and ROS levels (Fig. 1D, all $P<0.01$). Beyond that, the protein expression levels of SLC7A11 and GPX4 were lower in the MI/R group than in the Sham group (Fig. 1E, all $P<0.01$). These results suggested that the ferroptosis-related SLC7A11/GSH/GPX4 pathway played a protective role against I/R myocardial injury.

H/R induced ferroptosis in cardiomyocytes

Subsequently, we cultured rat cardiomyocytes H9C2 in vitro and established an H/R model Based on the CCK-8 and LDH assays, cell viability was repressed, while cell death was facilitated in the H/R group versus the Con

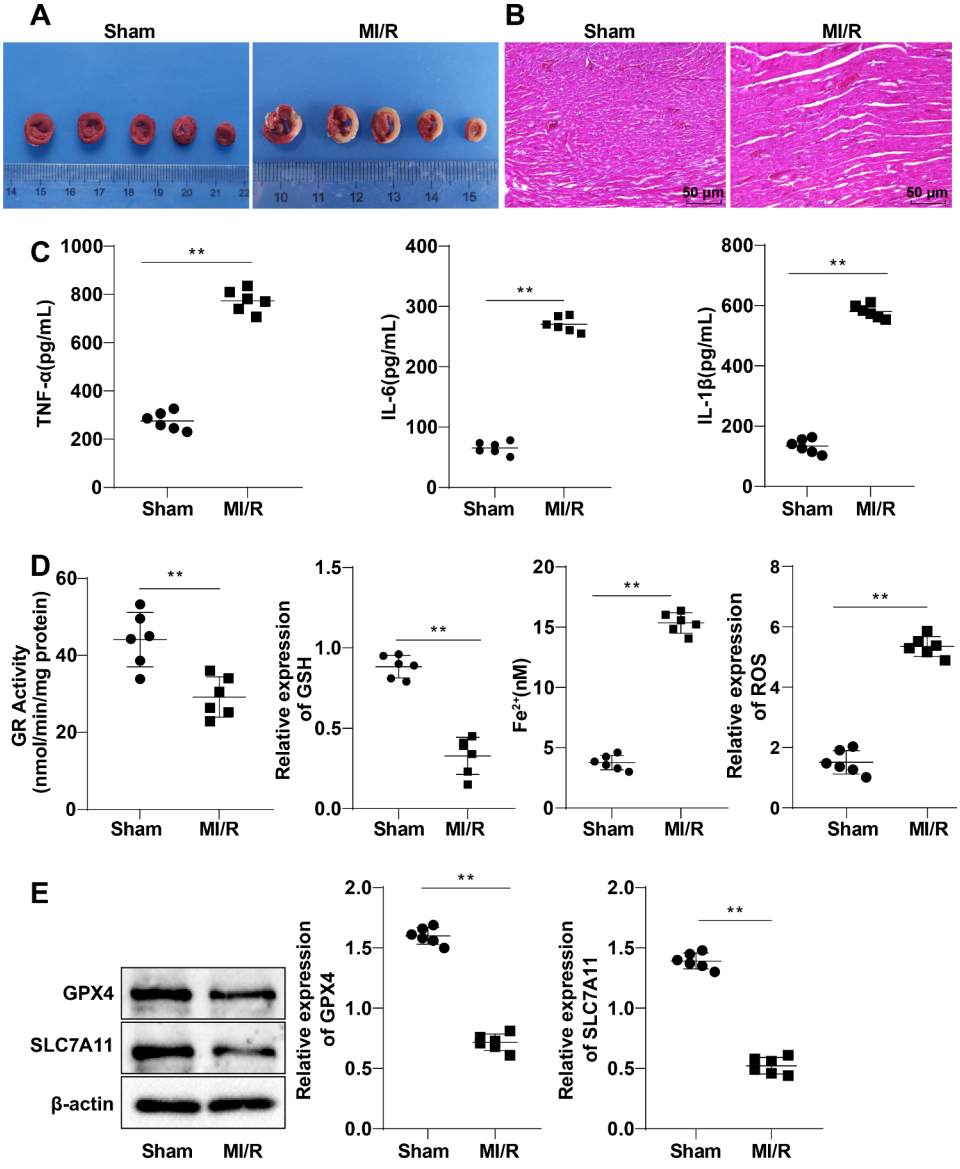

Fig. 1 I/R suppressed the ferroptosis-related SLC7A11/GSH/GPX4 pathway and induced myocardial injury. (**A**) TTC staining to detect the myocardial infarction area; (**B**) H&E staining to evaluate myocardial injury; (**C**) ELISA to determine the expression levels of TNF-α, IL-6 and IL-1β in myocardial tissues; (**D**) Detection of GR, GSH, Fe^{2+} and ROS levels in myocardial tissues using reagent kits; (**E**) Western blot to measure the expression level of SLC7A11 and GPX4 proteins. $n=6$. All experiments were repeated three times, and the data were expressed as mean ± standard deviation. An independent sample *t*-test was used to compare the data between the two groups. ** $P<0.01$. Full-length blots/gels are presented in the file named: Western Blots

group (Fig. 2A-B, all $P<0.01$). As reflected by ELISA, compared to the Con group, the expression levels of TNF-α, IL-6 and IL-1β in the H/R group were elevated (Fig. 2C, all $P<0.01$). Compared with the Con group, the levels of ROS, Fe^{2+}, MDA and LPO in the H/R group were raised (Fig. 2D-F, all $P<0.01$). The above results indicated that H/R induced ferroptosis in H9C2 cardiomyocytes. Subsequently, we treated H/R-induced H9C2 cells with ferroptosis inhibitor Lip-1. In contrast to the H/R+DMSO group, the H/R+Lip-1 group showed heightened cell viability, abated cell death, and diminished expression levels of TNF-α, IL-6, IL-1β, ROS, Fe^{2+}, MDA and LPO (Fig. 2A-F, all $P<0.05$). These findings further indicated that H/R induced ferroptosis in H9C2 cardiomyocytes.

H/R affected GSH synthesis and inhibited GPX4 enzyme activity by down-regulating SLC7A11

A study has found that SLC7A11 heightens the biosynthesis of GSH, while the lowered intracellular GSH levels can inactivate GSH-dependent GPX4, thus further potentiating ferroptosis [13, 31]. Therefore, we speculated that H/R inhibited GPX4 enzyme activity by down-regulating GSH. The expression level of SLC7A11 and GPX4

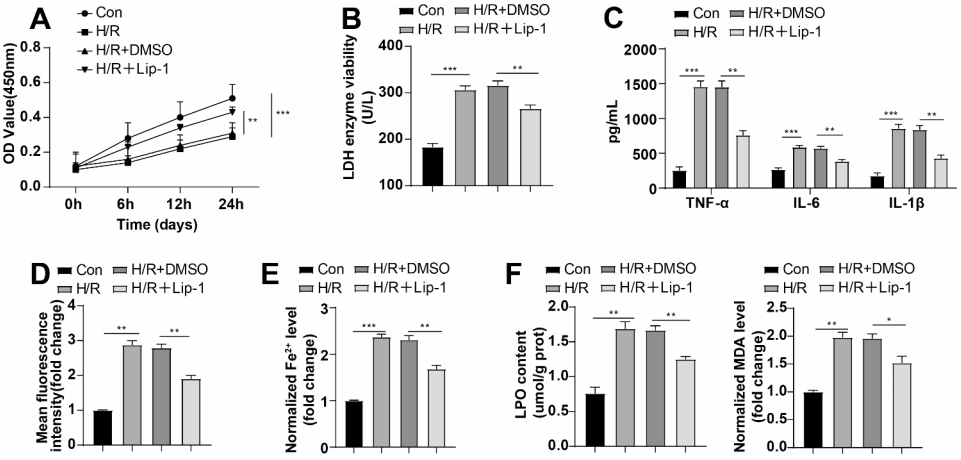

Fig. 2 H/R induced ferroptosis in cardiomyocytes. (**A**) CCK-8 assay to assess cell viability; (**B**) LDH assay to evaluate cell death; (**C**) ELISA to determine TNF-α, IL-6 and IL-1β expression levels; (**D**-**F**) The reagent kits were used to determine the levels of ROS, Fe^{2+}, MDA and LPO. The cell experiment was repeated three times, and the data were expressed as mean ± standard deviation. One-way ANOVA was used for inter-group data comparisons, and Tukey's multiple comparison test was used for post hoc testing. * $P<0.05$, ** $P<0.01$, *** $P<0.001$

proteins was diminished in the H/R group versus the Con group (Fig. 3A, all $P<0.05$). In comparison with the Con group, the GPX4 enzyme activity and levels of GSH, GSH/GSSH and GR in the H/R group dropped, whereas the GSSG level significantly rose (Fig. 3B/C, all $P<0.01$). Subsequently, cells were subjected to treatment with H/R oe-SLC7A11 and its NC. Higher levels of SLC7A11 and GPX4 protein expression, GPX4 enzyme activity and levels of GR, GSH and GSH/GSSH, along with lower levels of GSSG were observed in the H/R+oe-SLC7A11 group than in the H/R+oe-NC group (Fig. 3A-C, all $P<0.05$). Altogether, the above-mentioned results suggested that H/R affected the synthesis of GSH and suppressed GPX4 enzyme activity by down-regulating SLC7A11.

Upregulation of SLC7A11 ameliorated H/R-induced ferroptosis in cardiomyocytes via the GSH/GPX4 pathway

To verify the effect of the SLC7A11/GSH/GPX4 pathway on H/R-induced ferroptosis in cardiomyocytes, we treated cardiomyocytes with H/R and simultaneously overexpressed SLC7A11. Compared with the H/R+oe-NC group, the H/R+oe-SLC7A11 group showed elevated cell viability and lessened cell death, as well as diminished expression levels of TNF-α, IL-6, IL-1β, ROS, Fe^{2+}, MDA and LPO (Fig. 4A-F, all $P<0.01$). These results suggested that upregulation of SLC7A11 relieved H/R-induced ferroptosis in cardiomyocytes through the GSH/GPX4 pathway.

H/R activated mitophagy in cardiomyocytes

GPX4 is capable of inducing ferroptosis by means of mitophagy and mitochondrial damage and degradation stimulated by ROS [19]. To observe ROS-elicited mitophagy in cardiomyocytes under H/R conditions, we subjected cardiomyocytes to H/R treatment and 3-MA treatment. Through TEM, we observed that after H/R treatment, the outer membrane of mitochondria ruptured, mitochondrial cristae decreased, and mitochondrial membrane density increased. Nevertheless, compared to the H/R+DMSO group, the H/*R*+3-MA group showed a reduced degree of mitochondrial outer membrane rupture, increased mitochondrial cristae, and decreased mitochondrial membrane density (Fig. 5A). Moreover, MMP (ΔΨ) detection showed that relative to the Con group, the H/R group showed an upward trend in green fluorescence, and a downward trend in ΔΨ, whereas compared with the H/R+DMSO group, the H/*R*+3-MA group showed reduced green fluorescence and elevated ΔΨ (Fig. 5B, $P<0.01$). As reflected by Western blot, a higher LC3II/I protein level and a lower p62 protein level were observed in the H/R group than in the Con group, but the trends were opposite in the H/*R*+3-MA group versus the H/R+DMSO group (Fig. 5C, all $P<0.01$). The results suggested that H/R stimulated the activation of mitophagy in cardiomyocytes.

Activation of mitophagy partially reversed SLC7A11 overexpression-mediated improvement on H/R-induced ferroptosis in cardiomyocytes

We treated cardiomyocytes with oe-SLC7A11 or with both oe-SLC7A11 and rapamycin upon H/R treatment. Cells in the H/R+oe-SLC7A11 group showed less rupture of the outer mitochondrial membrane, more mitochondrial cristae, less mitochondrial membrane density, less green fluorescence, higher ΔΨ, a lower level of cellular LC3II/I protein, and a higher level of p62 protein than cells in the H/R+oe-NC group (Fig. 6A-C, all $P<0.01$). There were ruptured mitochondrial outer membrane, lessened mitochondrial cristae, increased mitochondrial membrane density, augmented green fluorescence

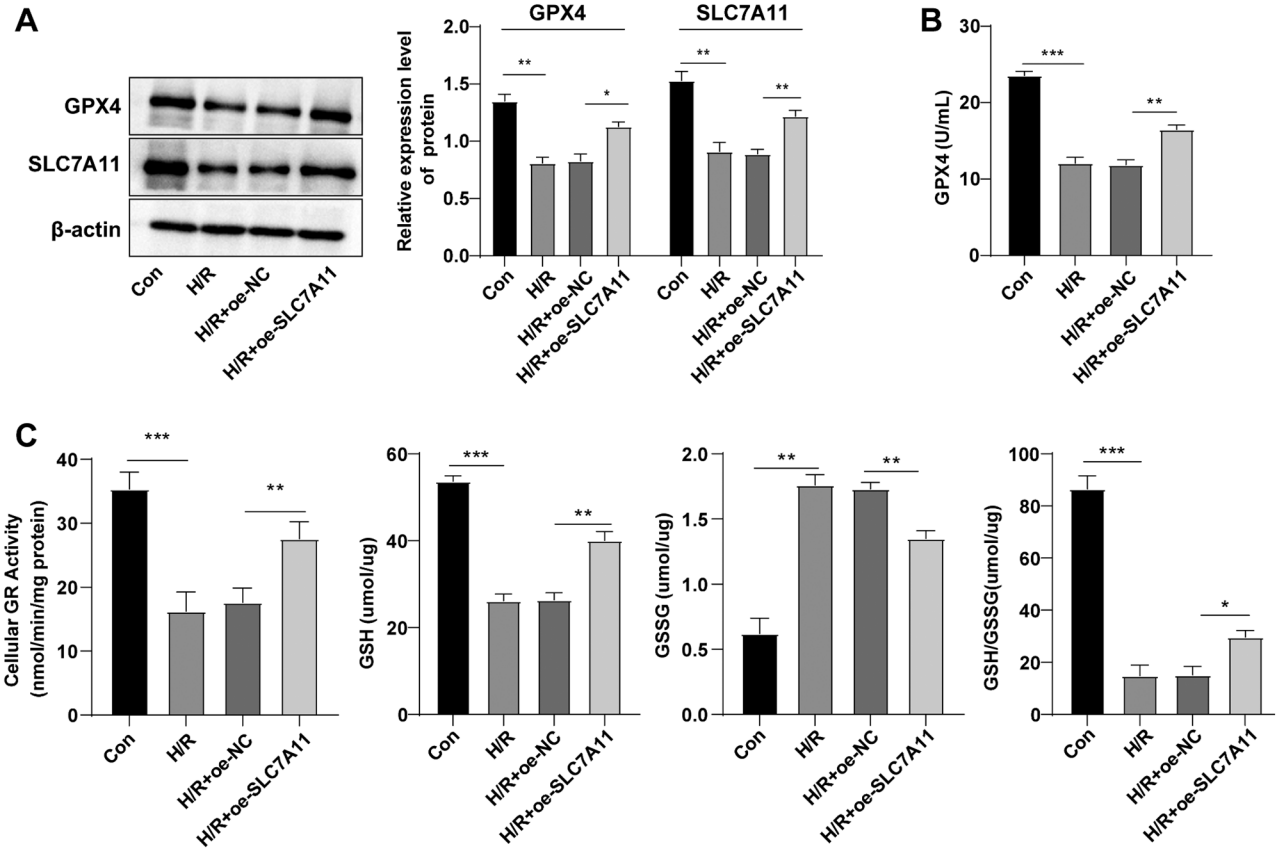

Fig. 3 H/R affected GSH synthesis and suppressed GPX4 enzyme activity by down-regulating SLC7A11. (**A**) Western blot to determine the expression of SLC7A11 and GPX4 protein. Full-length blots/gels are presented in the file named: Western Blots; (**B**-**C**) The reagent kits were used to measure the levels of GPX4, GR, GSH and GSSG. The experiment was repeated three times, and the data were expressed as mean ± standard deviation. One-way ANOVA was used for data comparisons between multiple groups, and Tukey's multiple comparison test was used for post hoc testing. * $P < 0.05$, ** $P < 0.01$, *** $P < 0.001$

emission, reduced ΔΨ, an elevated LC3II/I protein level, a lowered p62 protein level, abated cell viability, increased cell death, raised expression levels of inflammatory factors TNF-α, IL-6 and IL-1β, as well as ROS, Fe^{2+}, MDA and LPO in the H/R + oe-SLC7A11 + RA group versus the H/R + oe-SLC7A11 + DMSO group (Fig. 6A-I, all $P < 0.01$). These data suggested that activating mitophagy partially averted the improvement effect of SLC7A11 overexpression on H/R-induced ferroptosis in cardiomyocytes.

Discussion

MI/RI refers to the damage that occurs in the heart tissues as a result of the worsening of ischemia in the myocardium following the blockage of a coronary artery [32]. Currently, there are limited treatment options for MI/RI, and the resulting damage is typically irreversible. It has been established that genetic modifications in the ferroptosis pathway effectively impede ferroptosis and reduce myocardial damage [33]. Herein, our study sheds light on the molecular mechanisms of the ferroptosis-related SLC7A11/GSH/GPX4 pathway in MI/RI, providing avenues for the MI/RI development of future therapeutic strategies.

Inspiringly, ferroptosis has been identified to show significant involvement in cardiomyopathy, myocardial infarction, and MI/RI [34]. Suppressing SLC7A11 expression leads to reductions in GSH/GPX4 activity [35], while SLC7A11 and its downstream GPX4 or GSH are considered key modulatory genes in ferroptosis, and their downregulation indicates the occurrence of ferroptosis-related damage, such as myocardial injury [36–38]. Also, GPX4 and GSH levels are reduced with the development of myocardial infarction inhibiting GPX4 or GSH raises lipid ROS levels, which induces myocardial ferroptosis and myocardial damage [39]. In this study, we first created an MI/RI rat model and confirmed the protective role of the SLC7A11/GSH/GPX4 pathway in I/RI. Similarly, through the SIRT1/p53/SLC7A11 connection, USP22 overexpression may prevent ferroptosis-induced cardiomyocyte death and shield against MI/RI [40]. Dexmedetomidine post-conditioning mitigates cardiac I/RI in rats by inhibiting ferroptosis through the activation

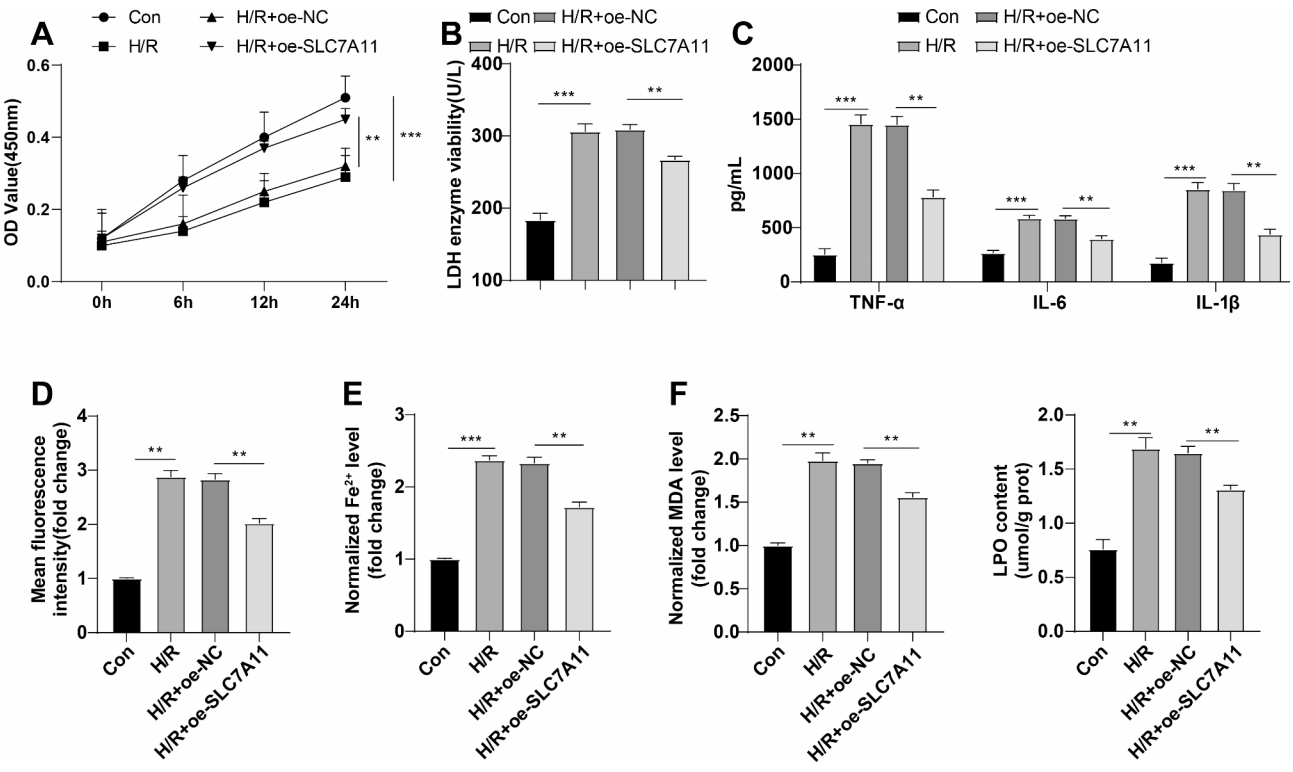

Fig. 4 Upregulation of SLC7A11 improved H/R-induced ferroptosis in cardiomyocytes through the GSH/GPX4 pathway. (**A**) CCK-8 assay to evaluate cell viability; (**B**) LDH detection method was used to assess cell death; (**C**) ELISA to determine the expression levels of TNF-α, IL-6 and IL-1β; (**D**-**F**) The reagent kits were used to determine the levels of ROS, Fe^{2+}, MDA and LPO. The experiment was repeated three times, and the data were expressed as mean ± standard deviation. One-way ANOVA was employed for data comparisons between multiple groups, and Tukey's multiple comparison test was used for post hoc testing. ** $P < 0.01$, *** $P < 0.001$

of the SLC7A11/GPX4 axis [41]. Zhang et al. have also revealed that hydrogen sulfide can prevent cardiomyocytes from oxidative stress and protect against cardiotoxicity by reducing doxorubicin-induced ferroptosis through the SLC7A11/GSH/GPX4 antioxidant pathway [42].

Subsequently, we cultured H9C2 rat cardiomyocytes in vitro and created an H/R model. Not surprisingly, it was discovered that H/R could stimulate ferroptosis in H9C2 cardiomyocytes, which was also mentioned in published reports [43, 44]. In addition to this, we also observed that further treatment of oe-SLC7A11 transfection in H/R-treated cells heightened SLC7A11, GPX4, GR, GSH and GSH/GSSH levels, and GPX4 enzyme activity, as well as decreased GSSG level in H9C2 cells. SLC7A11 repression abates GSH level and subsequently lowers GPX4 enzyme activity, which provokes cellular/subcellular membranes or ferroptosis [34, 45]. Consequently, H/R affected the synthesis of GSH and suppressed GPX4 enzyme activity via the downregulation of SLC7A11. Similar to our results, reduced ROS and Fe^{2+} levels and suppressed cardiac ferroptosis are achieved by overexpressing SLC7A11 in cardiomyocytes [46]. Additionally, Fang et al. reported that ferritin H-deficient cardiomyocytes have decreased expression of the ferroptosis regulator SLC7A11, whereas upregulating SLC7A11 specifically in cardiomyocytes enhances GSH levels and effectively prevents cardiac ferroptosis [46]. Conversely, the ferroptosis inhibitor ferrostatin-1 partially reversed the negative effects of triptolide on the SLC7A11/GPX4 signal, thereby reducing triptolide-elicited cardiotoxicity [47]. Of importance, our findings unearthed that SLC7A11 could potentially be developed into a new therapeutic target in MI/RI. It is interesting to note that upregulation of SLC7A11 ameliorates H/R-induced cardiomyocyte ferroptosis via the GSH/GPX4 signaling pathway.

It has been reported that the suppression of SLC7A11 leads to GSH depletion, which in turn facilitates GPX4 inactivation [48]. Diminished SLC7A11 expression and the consequent decline in GSH and GPX4 levels play a crucial role in myocardial ferroptosis and cardiomyopathy [47]. In addition, GPX4 can stimulate ferroptosis by promoting mitophagy and ROS-induced mitochondrial damage and degradation [19]. However, the regulatory role of SLC7A11 in mitophagy has been scarcely reported. Thus, we further investigated the interaction between SLC7A11 and cardiomyocyte mitophagy. We added the mitophagy inhibitor 3-MA to treat H/R-induced H9C2 cells. Based on the results, 3-MA inhibited H/R-induced mitophagy in H9C2 cells and the

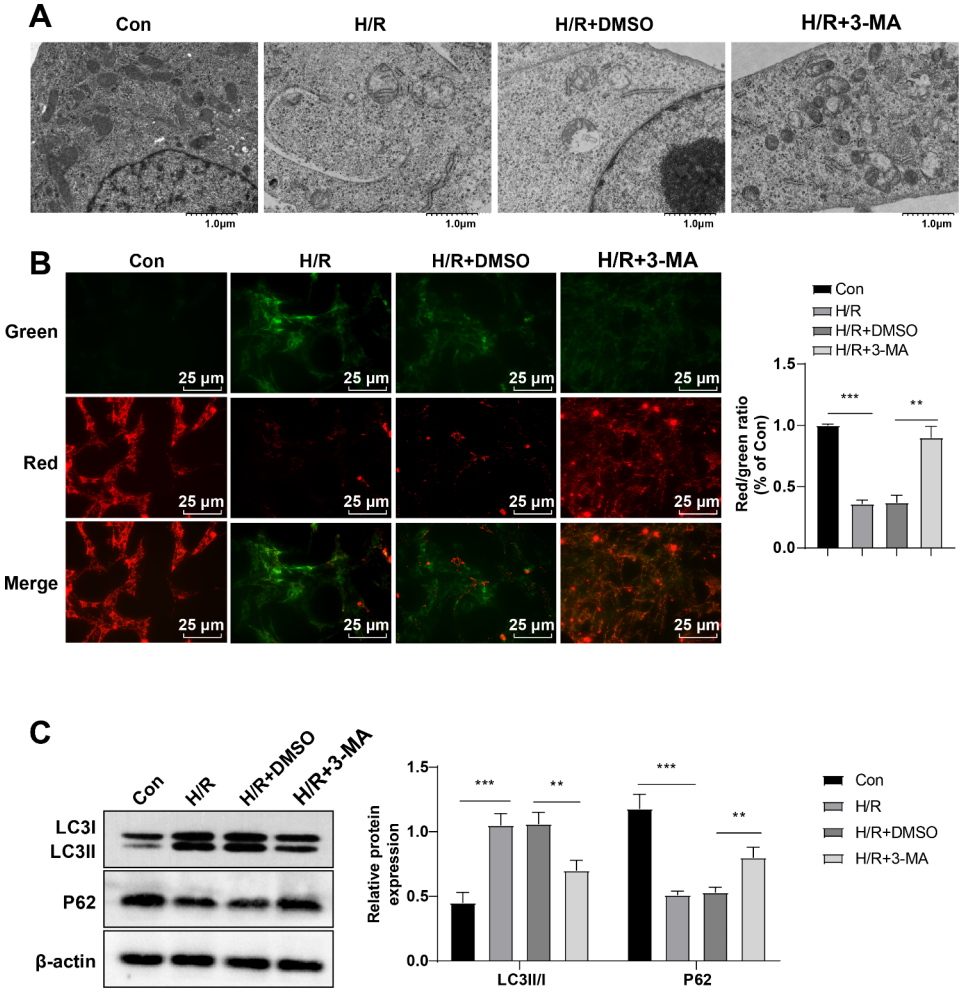

Fig. 5 H/R activated mitophagy in cardiomyocytes. (**A**) Observation of mitochondrial morphology using a TEM; (**B**) Fluorescent dye JC-1 was used to detect MMP (ΔΨ); (**C**) Western blot to assess the expression level of LC3II/I and p62 proteins. The experiment was repeated three times, and the data were expressed as mean ± standard deviation. One-way ANOVA was used for data comparisons between multiple groups, followed by Tukey's multiple comparison test. ** $P < 0.01$, *** $P < 0.001$. Full-length blots/gels are presented in the file named: Western Blots

activation of mitophagy partially reversed the ameliorative effect of SLC7A11 upregulation on H/R-induced ferroptosis in cardiomyocytes. Accordingly, increased ROS under H/R conditions induced myocardial injury by inducing mitophagy to curb the activation of the ferroptosis-related SLC7A11/GSH/GPX4 pathway. A previous study has reported that 3-MA can mitigate myocardial injury in MI/RI rats [49]. Also, the autophagy inhibitor 3-MA has the potential to reduce cardiac damage caused by excessive exercise in rats [50]. 3-MA improves the exacerbated I/R-induced heart damage and dysfunction in the group administered with nicotine compared to the control group [51]. As a result, the mitophagy inhibitor 3-MA may be promising for clinical application in the treatment of ischemic heart disease. Furthermore, the ferroptosis inhibitor Lip-1 has been documented to protect the mouse myocardium against I/RI [52]. Meanwhile, treatment with Lip-1 results in increased viability and decreased death of H/R cells, and reduces the level of inflammatory factors, which provides a theoretical basis for the development of ferroptosis-related reagents for myocardial injury in the clinic, but still needs to be further explored. Another noteworthy observation in our study was that the transfection of oe-SLC7A11 in H/R rats led to increased mitochondrial cristae, ΔΨ, and p62 protein level and decreased mitochondrial membrane density, green fluorescence, and LC3II/I protein level. To the best of our knowledge, we found for the first time that H/R could activate mitophagy in cardiomyocytes by suppressing the SLC7A11/GSH/GPX4 axis. Additionally, the improvement mediated by SLC7A11 upregulation on H/R-induced ferroptosis in cardiomyocytes could be partially annulled by mitophagy activation.

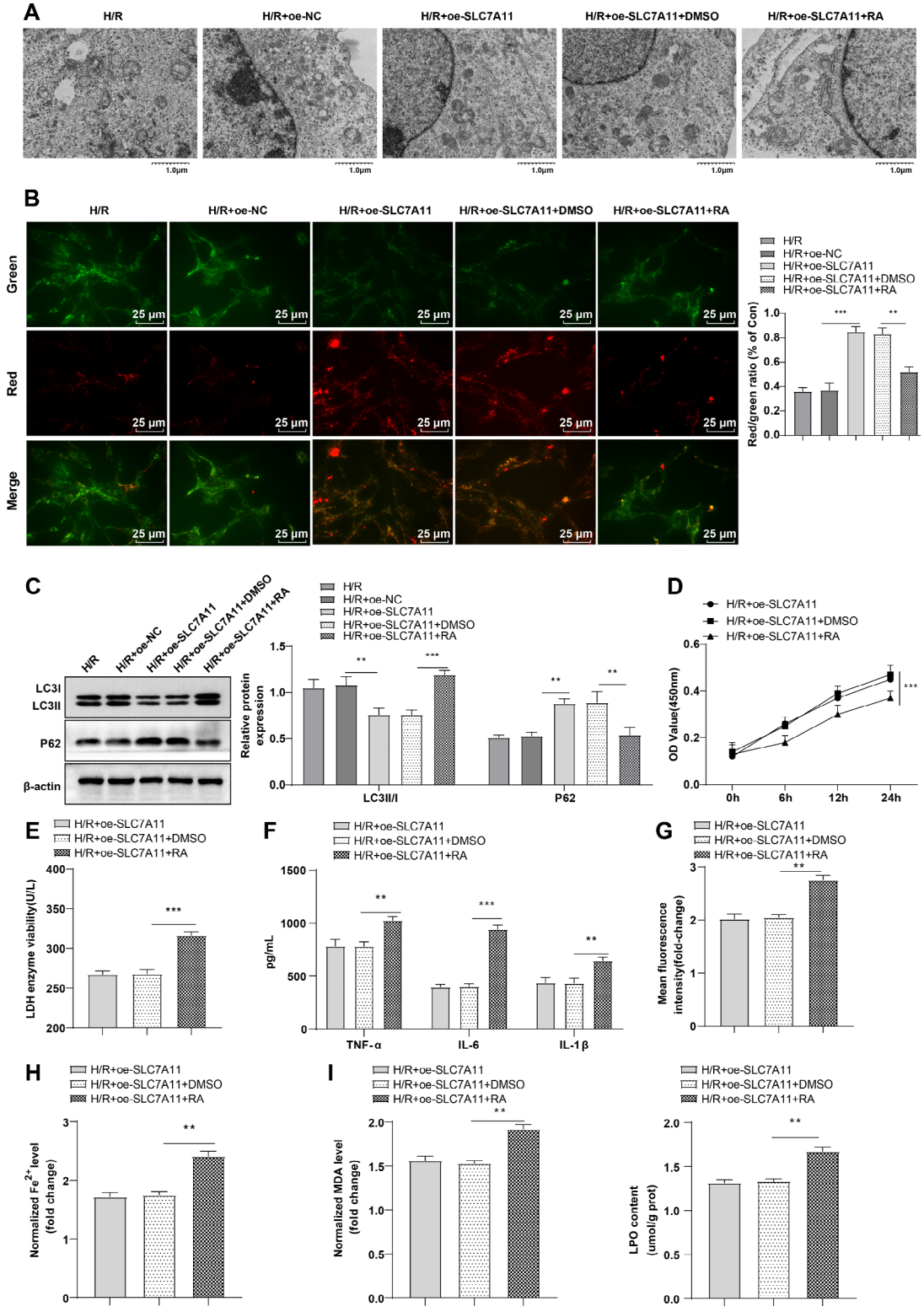

Fig. 6 Activation of mitophagy partially reversed SLC7A11 overexpression-mediated improvement on H/R-induced ferroptosis in cardiomyocytes. (**A**) Observation of mitochondrial morphology using a TEM; (**B**) Fluorescent dye JC-1 to detect MMP (ΔΨ); (**C**) Western blot to determine the expression levels of LC3II/I and p62 proteins. Full-length blots/gels are presented in the file named: Western Blots; (**D**) CCK-8 assay to evaluate cell viability; (**E**) LDH detection method to assess cell death; (**F**) ELISA to determine TNF-α, IL-6 and IL-1β expression levels; (**G**-**I**) The reagent kits to measure the levels of ROS, Fe^{2+}, MDA and LPO. The experiment was repeated three times, and the data were expressed as mean ± standard deviation. One-way ANOVA was adopted for data comparisons between multiple groups, followed by Tukey's multiple comparison test. ** $P < 0.01$, *** $P < 0.001$

Conclusions

The present study expounded that MI/RI limited the ferroptosis-related SLC7A11/GSH/GPX4 pathway, activated mitophagy in cardiomyocytes, and caused Fe^{2+} accumulation and LPO in cardiomyocytes, hence inducing myocardial injury. However, for this study, only the H9C2 cardiomyocyte cell line was chosen for investigation, with no additional cell lines included for more comprehensive analysis, and no clinical research carried out. It is believed that there will be clinical validation in the field of ferroptosis-related research in the future. In addition, further investigation is needed to explore the upstream and downstream target genes of the SLC7A11/GSH/GPX4 pathway, as well as other associated pathways.

Abbreviations

MI/RI	Myocardial ischemia-reperfusion injury
H/R	Hypoxia/reoxygenation
ROS	Reactive oxygen species
Nrf2	Nuclear factor erythroid-2
GSH	Related factor 2 Glutathione
GPX4	Glutathione peroxidase 4
TTC	2,3,5-triphenyl tetrazolium chloride staining
H&E	Hematoxylin and eosin staining
ELISA	Enzyme-linked immunosorbent assay
DMEM	Dulbecco's modified Eagle medium
DMSO	Dimethyl sulfoxide
CCK-8	Cell counting kit-8
OD	Optical density
LDH	Lactate dehydrogenase
MDA	Malondialdehyde
LPO	Lipid peroxidation
TEM	Transmission electron microscopy
MMP	Mitochondrial membrane potential
ANOVA	Analysis of variance
3-MA	3-Methyladenine

Supplementary Information

The online version contains supplementary material available at https://doi.org/10.1186/s12872-024-04220-3.

Supplementary Material 1

Acknowledgements

Not applicable.

Author contributions

Conceptualization, Ping Fan; Methodology, Ping Fan; Software, Mingjun Duan; Validation, Bingxin Chen, Xue Song and Mingjun Duan; Formal Analysis, Bingxin Chen and Ping Fan; Investigation, Bingxin Chen; Resources, Ping Fan; Data Curation, Bingxin Chen; Writing – Original Draft Preparation, Bingxin Chen; Writing – Review & Editing, Mingjun Duan; Visualization, Xue Song; Supervision, Xue Song; Project Administration, Mingjun Duan; Funding Acquisition, Bingxin Chen.

Funding

This research was supported by grants from Provincial and Ministry jointly built State Key Laboratory of Pathogenesis, Prevention, Treatment of Central Asian High Incidence Diseases Fund (SKL-HIDCA-2017-Y11; SKL-HIDCA-2024-40).

Data availability

All data generated or analysed during this study are included in this article. Further enquiries can be directed to the corresponding author.

Declarations

Ethics approval and consent to participate

All experimental protocols were reviewed and approved by the Research and Ethics Committee of the First Affiliated Hospital of Xinjiang Medical University. All procedures conformed to internationally accepted guidelines and ethics for animal research. All authors confirm that all methods are reported in accordance with ARRIVE guidelines for the reporting of animal experiments. Great efforts were made to reduce the total number of animals used and to minimize their suffering.

Consent for publication

Not applicable.

Competing interests

The authors declare no competing interests.

Author details

[1]Department of Cardiac Function, The First Affiliated Hospital of Xinjiang Medical University, No. 137 Liyushan South Road, High-tech District, Urumqi, Xinjiang Uygur Autonomous Region 830054, China
[2]State Key Laboratory of Pathogenesis, Prevention and Treatment of High Incidence Diseases in Central Asia, Animal Experimental Center of Xinjiang Medical University, No. 137 Liyushan South Road, High-tech District, Urumqi, Xinjiang Uygur Autonomous Region 830000, China
[3]State Key Laboratory of Pathogenesis, Prevention and Treatment of High Incidence Diseases in Central Asia, Urumqi, Xinjiang Uygur Autonomous Region, China

Received: 5 March 2024 / Accepted: 23 September 2024
Published online: 01 October 2024

References

1. Xu S, Wu B, Zhong B, Lin L, Ding Y, Jin X, et al. Naringenin alleviates myocardial ischemia/reperfusion injury by regulating the nuclear factor-erythroid factor 2-related factor 2 (Nrf2) /System xc-/ glutathione peroxidase 4 (GPX4) axis to inhibit ferroptosis. Bioengineered. 2021;12(2):10924–34.
2. Mao ZJ, Lin H, Hou JW, Zhou Q, Wang Q, Chen YH. A Meta-analysis of Resveratrol protects against Myocardial Ischemia/Reperfusion Injury: evidence from Small Animal studies and Insight into Molecular mechanisms. Oxid Med Cell Longev. 2019;2019:5793867.
3. Wang J, Xu RM, Cao QM, Ma BC, Zhang H, Hao HP. Mechanism of DYRK1a in myocardial ischemia-reperfusion injury by regulating ferroptosis of cardiomyocytes. Kaohsiung J Med Sci. 2023;39(12):1190–9.
4. Zhang H, Yin Y, Liu Y, Zou G, Huang H, Qian P, et al. Necroptosis mediated by impaired autophagy flux contributes to adverse ventricular remodeling after myocardial infarction. Biochem Pharmacol. 2020;175:113915.
5. Yang T, Liu H, Yang C, Mo H, Wang X, Song X, et al. Galangin attenuates myocardial ischemic reperfusion-Induced ferroptosis by targeting Nrf2/Gpx4 signaling pathway. Drug Des Devel Ther. 2023;17:2495–511.
6. Wang Z, Yang N, Hou Y, Li Y, Yin C, Yang E, et al. L-Arginine-loaded gold nanocages ameliorate myocardial Ischemia/Reperfusion Injury by promoting nitric oxide production and maintaining mitochondrial function. Adv Sci (Weinh). 2023;10(26):e2302123.
7. Kroemer G, Levine B. Autophagic cell death: the story of a misnomer. Nat Rev Mol Cell Biol. 2008;9(12):1004–10.
8. Dixon SJ, Lemberg KM, Lamprecht MR, Skouta R, Zaitsev EM, Gleason CE, et al. Ferroptosis: an iron-dependent form of nonapoptotic cell death. Cell. 2012;149(5):1060–72.
9. Gao M, Monian P, Quadri N, Ramasamy R, Jiang X. Glutaminolysis and transferrin regulate Ferroptosis. Mol Cell. 2015;59(2):298–308.
10. Fang X, Wang H, Han D, Xie E, Yang X, Wei J, et al. Ferroptosis as a target for protection against cardiomyopathy. Proc Natl Acad Sci U S A. 2019;116(7):2672–80.

11. Yan J, Li Z, Liang Y, Yang C, Ou W, Mo H, et al. Fucoxanthin alleviated myocardial ischemia and reperfusion injury through inhibition of ferroptosis via the NRF2 signaling pathway. Food Funct. 2023;14(22):10052–68.
12. Xu G, Wang H, Li X, Huang R, Luo L. Recent progress on targeting ferroptosis for cancer therapy. Biochem Pharmacol. 2021;190:114584.
13. Koppula P, Zhang Y, Zhuang L, Gan B. Amino acid transporter SLC7A11/xCT at the crossroads of regulating redox homeostasis and nutrient dependency of cancer. Cancer Commun (Lond). 2018;38(1):12.
14. Hu K, Li K, Lv J, Feng J, Chen J, Wu H, et al. Suppression of the SLC7A11/glutathione axis causes synthetic lethality in KRAS-mutant lung adenocarcinoma. J Clin Invest. 2020;130(4):1752–66.
15. Chen W, Zhang Y, Wang Z, Tan M, Lin J, Qian X, et al. Dapagliflozin alleviates myocardial ischemia/reperfusion injury by reducing ferroptosis via MAPK signaling inhibition. Front Pharmacol. 2023;14:1078205.
16. Klionsky DJ, Emr SD. Autophagy as a regulated pathway of cellular degradation. Science. 2000;290(5497):1717–21.
17. Zhang M, Tong Z, Wang Y, Fu W, Meng Y, Huang J, et al. Relationship between ferroptosis and mitophagy in renal fibrosis: a systematic review. J Drug Target. 2023;31(8):858–66.
18. Liu M, Fan Y, Li D, Han B, Meng Y, Chen F, et al. Ferroptosis inducer erastin sensitizes NSCLC cells to celastrol through activation of the ROS-mitochondrial fission-mitophagy axis. Mol Oncol. 2021;15(8):2084–105.
19. Bi Y, Liu S, Qin X, Abudureyimu M, Wang L, Zou R, et al. FUNDC1 interacts with GPx4 to govern hepatic ferroptosis and fibrotic injury through a mitophagy-dependent manner. J Adv Res. 2024;55:45–60.
20. Liu W, Chen C, Gu X, Zhang L, Mao X, Chen Z, et al. AM1241 alleviates myocardial ischemia-reperfusion injury in rats by enhancing Pink1/Parkin-mediated autophagy. Life Sci. 2021;272:119228.
21. Huang ZQ, Xu W, Wu JL, Lu X, Chen XM. MicroRNA-374a protects against myocardial ischemia-reperfusion injury in mice by targeting the MAPK6 pathway. Life Sci. 2019;232:116619.
22. Han RH, Huang HM, Han H, Chen H, Zeng F, Xie X, et al. Propofol postconditioning ameliorates hypoxia/reoxygenation induced H9c2 cell apoptosis and autophagy via upregulating forkhead transcription factors under hyperglycemia. Mil Med Res. 2021;8(1):58.
23. Li D, Wang Y, Dong C, Chen T, Dong A, Ren J, et al. CST1 inhibits ferroptosis and promotes gastric cancer metastasis by regulating GPX4 protein stability via OTUB1. Oncogene. 2023;42(2):83–98.
24. Pi Y, Tian X, Ma J, Zhang H, Huang X. Vitamin D alleviates hypoxia/reoxygenation-induced injury of human trophoblast HTR-8 cells by activating autophagy. Placenta. 2021;111:10–8.
25. Singh A, Wilson JW, Schofield CJ, Chen R. Hypoxia-inducible factor (HIF) prolyl hydroxylase inhibitors induce autophagy and have a protective effect in an in-vitro ischaemia model. Sci Rep. 2020;10(1):1597.
26. Welles JE, Dennis MD, Jefferson LS, Kimball SR. Glucagon-dependent suppression of mTORC1 is Associated with Upregulation of hepatic FGF21 mRNA translation. Am J Physiol Endocrinol Metab. 2020;319(1):E26–33.
27. Ornelas IM, Khandker L, Wahl SE, Hashimoto H, Macklin WB, Wood TL. The mechanistic target of rapamycin pathway downregulates bone morphogenetic protein signaling to promote oligodendrocyte differentiation. Glia. 2020;68(6):1274–90.
28. Li Y, Sun X, Zhuang J, Wang J, Yang C. Donepezil ameliorates oxygen–glucose deprivation/reoxygenation–induced cardiac microvascular endothelial cell dysfunction through PARP1/NF–kappaB signaling. Mol Med Rep. 2022;25(4).
29. Zhang Z, Cui S, Fu Y, Wang J, Liu J, Wei F. Mechanical force induces mitophagy-mediated anaerobic oxidation in periodontal ligament stem cells. Cell Mol Biol Lett. 2023;28(1):57.
30. Busa P, Lee SO, Huang N, Kuthati Y, Wong CS. Carnosine alleviates knee osteoarthritis and promotes Synoviocyte Protection via activating the Nrf2/HO-1 signaling pathway: an In-Vivo and In-Vitro Study. Antioxid (Basel). 2022;11(6).
31. Nagasaki T, Schuyler AJ, Zhao J, Samovich SN, Yamada K, Deng Y et al. 15LO1 dictates glutathione redox changes in asthmatic airway epithelium to worsen type 2 inflammation. J Clin Invest. 2022;132(1).
32. Li Y, Zhang H, Li Z, Yan X, Li Y, Liu S. microRNA-130a-5p suppresses myocardial ischemia reperfusion injury by downregulating the HMGB2/NF-kappaB axis. BMC Cardiovasc Disord. 2021;21(1):121.
33. Huang F, Yang R, Xiao Z, Xie Y, Lin X, Zhu P, et al. Targeting ferroptosis to treat Cardiovascular diseases: a New Continent to be explored. Front Cell Dev Biol. 2021;9:737971.
34. Wu X, Li Y, Zhang S, Zhou X. Ferroptosis as a novel therapeutic target for cardiovascular disease. Theranostics. 2021;11(7):3052–9.
35. Katunga LA, Gudimella P, Efird JT, Abernathy S, Mattox TA, Beatty C, et al. Obesity in a model of gpx4 haploinsufficiency uncovers a causal role for lipid-derived aldehydes in human metabolic disease and cardiomyopathy. Mol Metab. 2015;4(6):493–506.
36. Zhao MY, Liu P, Sun C, Pei LJ, Huang YG. Propofol augments Paclitaxel-Induced Cervical Cancer Cell Ferroptosis in Vitro. Front Pharmacol. 2022;13:816432.
37. Tan M, Yin Y, Ma X, Zhang J, Pan W, Tan M, et al. Glutathione system enhancement for cardiac protection: pharmacological options against oxidative stress and ferroptosis. Cell Death Dis. 2023;14(2):131.
38. Chen Y, Deng Y, Chen L, Huang Z, Yan Y, Huang Z. Mir-16-5p regulates ferroptosis by Targeting SLC7A11 in Adriamycin-Induced ferroptosis in Cardiomyocytes. J Inflamm Res. 2023;16:1077–89.
39. Park TJ, Park JH, Lee GS, Lee JY, Shin JH, Kim MW, et al. Quantitative proteomic analyses reveal that GPX4 downregulation during myocardial infarction contributes to ferroptosis in cardiomyocytes. Cell Death Dis. 2019;10(11):835.
40. Ma S, Sun L, Wu W, Wu J, Sun Z, Ren J. USP22 protects against myocardial ischemia-reperfusion Injury via the SIRT1-p53/SLC7A11-Dependent inhibition of Ferroptosis-Induced Cardiomyocyte Death. Front Physiol. 2020;11:551318.
41. Yu P, Zhang J, Ding Y, Chen D, Sun H, Yuan F, et al. Dexmedetomidine post-conditioning alleviates myocardial ischemia-reperfusion injury in rats by ferroptosis inhibition via SLC7A11/GPX4 axis activation. Hum Cell. 2022;35(3):836–48.
42. Zhang H, Pan J, Huang S, Chen X, Chang ACY, Wang C, et al. Hydrogen sulfide protects cardiomyocytes from doxorubicin-induced ferroptosis through the SLC7A11/GSH/GPx4 pathway by Keap1 S-sulfhydration and Nrf2 activation. Redox Biol. 2024;70:103066.
43. Liu XJ, Lv YF, Cui WZ, Li Y, Liu Y, Xue YT, et al. Icariin inhibits hypoxia/reoxygenation-induced ferroptosis of cardiomyocytes via regulation of the Nrf2/HO-1 signaling pathway. FEBS Open Bio. 2021;11(11):2966–76.
44. Geng W, Yan S, Li X, Liu Q, Zhang X, Gu X, et al. Mir-432-5p inhibits the ferroptosis in Cardiomyocytes Induced by Hypoxia/Reoxygenation via activating Nrf2/SLC7A11 Axis by Degrading Keap1. Anal Cell Pathol (Amst). 2023;2023:1293200.
45. Wu G, Fang YZ, Yang S, Lupton JR, Turner ND. Glutathione metabolism and its implications for health. J Nutr. 2004;134(3):489–92.
46. Fang X, Cai Z, Wang H, Han D, Cheng Q, Zhang P, et al. Loss of Cardiac Ferritin H facilitates Cardiomyopathy via Slc7a11-Mediated ferroptosis. Circ Res. 2020;127(4):486–501.
47. Liu X, Chen C, Han D, Zhou W, Cui Y, Tang X, et al. SLC7A11/GPX4 inactivation-mediated ferroptosis contributes to the pathogenesis of Triptolide-Induced Cardiotoxicity. Oxid Med Cell Longev. 2022;2022:3192607.
48. Dai C, Chen X, Li J, Comish P, Kang R, Tang D. Transcription factors in ferroptotic cell death. Cancer Gene Ther. 2020;27(9):645–56.
49. Zhang HR, Bai H, Yang E, Zhong ZH, Chen WY, Xiao Y, et al. Effect of moxibustion preconditioning on autophagy-related proteins in rats with myocardial ischemia reperfusion injury. Ann Transl Med. 2019;7(20):559.
50. Liu H, Lei H, Shi Y, Wang JJ, Chen N, Li ZH, et al. Autophagy inhibitor 3-methyladenine alleviates overload-exercise-induced cardiac injury in rats. Acta Pharmacol Sin. 2017;38(7):990–7.
51. Zhang P, Li Y, Fu Y, Huang L, Liu B, Zhang L, et al. Inhibition of Autophagy Signaling via 3-methyladenine rescued nicotine-mediated Cardiac Pathological effects and Heart dysfunctions. Int J Biol Sci. 2020;16(8):1349–62.
52. Feng Y, Madungwe NB, Imam Aliagan AD, Tombo N, Bopassa JC. Liproxstatin-1 protects the mouse myocardium against ischemia/reperfusion injury by decreasing VDAC1 levels and restoring GPX4 levels. Biochem Biophys Res Commun. 2019;520(3):606–11.

Publisher's note